

A Study of the Chemical Composition of Cosmic Rays Around 10^{18} eV

We compare the depth of maximum distribution of showers observed by the Fly's Eye detector to the results of detailed Monte Carlo calculations, including detector efficiency and reconstruction errors. The comparison shows that the cosmic ray composition in the region of 10^{18} eV is quite heavy. Nuclei of mass > 20 comprise about 80% of the cosmic ray flux at $\sim 5 \times 10^{17}$ eV. At higher energy we observe a light (H + He) component, characterized by a relatively flat energy spectrum, which is consistent with some models of acceleration of ultra-high energy cosmic rays, and may signal the emergence of an extragalactic cosmic ray component.

1. INTRODUCTION

The energy range under consideration, around 10^{18} eV/nucleus, lies in a smooth part of the cosmic ray spectrum, between its two main features: "the knee" at $\sim 5 \times 10^{15}$ eV, where the differential spectrum steepens from $E^{-2.7}$ to approximately $E^{-3.1}$, and "the ankle" above 10^{19} eV, where the spectrum may flatten again. The common wisdom is that "the knee" marks the energy where galactic sources of cosmic rays become less efficient in particle acceleration, and that "the ankle" is due to extragalactic cosmic ray flux. A measurement of the composition of the cosmic ray flux at this energy could then be relevant both to the higher end of the galactic component and the lower end of the extragalactic component of the cosmic rays. It can contribute towards answering some important astrophysical questions, such as the nature of the

Comments Astrophys.
1993, Vol. 17, Nos. 2 & 3, pp. 103–117
Reprints available directly from the publisher
Photocopying permitted by license only

© 1993 Gordon and Breach,
Science Publishers SA
Printed in Malaysia

galactic sources of very high energy cosmic rays, the general structure and strength of galactic magnetic fields, and the power that luminous extragalactic objects emit in the form of nuclei.

In the 10^9 – 10^{11} eV energy range the composition of cosmic rays is well measured and understood. It is dominated by H, He and other light nuclei. The recent measurements^{1–3} at higher energy, which extend to 10^{14} eV/nucleus,* show that the energy spectra of medium and heavy nuclei are flatter than those of H and He and the cosmic ray composition has changed significantly. Around 10^{14} eV/nucleus the flux could be represented⁴ as the sum of five components (H, He, C–O, Ne–S, and $Z > 17$) that contribute approximately equally to the total particle flux, which becomes increasingly heavy.

The derivation of the chemical composition at higher energy from air shower data has failed to provide a consistent result. While some types of experiments and analyses^{5–7} derive a proton dominated composition, others^{8–11} see the continuation of the trend toward heavier composition observed by direct experiments.

A heavier composition at higher energies is not unexpected since the accepted acceleration model—diffusive shock acceleration^{12,13}—has a maximum rigidity which implies a mass dependent maximum energy E_{\max} . After the accelerator is exhausted for singly charged H nuclei, only higher Z nuclei can be accelerated. Supernova blast shocks in the interstellar medium, believed to be the source of the bulk of cosmic rays, cannot accelerate particles to energies above $E_{\max} \sim 10^{14}$ eV $\times Z$.¹² The existence of cosmic rays above these energies requires either a different class of acceleration sites or reacceleration on a larger spatial scale. With a few notable exceptions^{15,16} mechanisms of cosmic ray sources at higher energies also use rigidity dependent diffusive shock acceleration, which suggests a second transition from light to heavy composition for this new component.

In this paper we report on a measurement of cosmic ray composition through analysis of giant air showers detected by the Fly's Eye.¹⁷ In Section 2 we give a brief outline of the experimental

*We discuss here the cosmic ray flux in terms of energy/nucleus, since air showers reflect the total energy of the cosmic ray nuclei.

technique and the data analysis. In Section 3 we summarize the experimental results on the cosmic ray composition around 10^{18} eV/nucleus and then discuss their astrophysical implications and evaluate parameters in different models of the cosmic ray origin in Section 4.

2. EXPERIMENTAL TECHNIQUE AND DATA ANALYSIS

An air shower commences when a high energy cosmic ray particle interacts inelastically in the atmosphere and produces multiple secondary hadrons. A cascade develops and reaches its maximum size (number of charged particles) at an energy-dependent atmospheric depth $X_{\max} \propto \ln(E_0/A)$. The cascade then attenuates as particles stop due to ionization energy loss. For primary nuclei of energy 10^{18} eV the number of charged particles at shower maximum, most of them electrons, is close to 10^9 . The sensitivity of the shower development to the cosmic ray composition comes from the different rates of energy dissipation in showers initiated by primaries of different mass. Showers generated by heavy nuclei develop faster and reach X_{\max} at shallower atmospheric depths. At 10^{18} eV, the average X_{\max} for proton showers is about 100 g/cm² larger than for iron showers.

Unlike other shower experiments, which study the air shower characteristics only at the Earth's surface, the Fly's Eye observes the longitudinal development of the air showers. The charged shower particles excite the nitrogen atoms in the atmosphere and cause fluorescence emission of approximately 4 photons per meter per electron. The light is observed at the ground by multiple mirror/photomultiplier systems at two locations separated by 3.4 km. A geometrical reconstruction then determines the amount of light emitted at different atmospheric depths along the shower trajectory, which is a measure of the number of charged particles at those depths. The integral of shower size with respect to atmospheric depth is proportional to the primary energy E_0 , as is N_{\max} , the number of shower particles at X_{\max} . Thus both X_{\max} and E_0 are measured in a direct way which is not possible for a ground array. In contrast to the showers' Cherenkov radiation, the scin-

tillation light is emitted isotropically, allowing very remote detection of showers over areas of hundreds of square kilometers.

The current Fly's Eye configuration consists of Fly's Eye I with 67 mirrors and a total of 880 phototubes and Fly's Eye II with 36 mirrors and 464 phototubes. A technical description of the detector is given in Ref. 18.

The idea of the data analysis is to simulate showers generated by primaries of different mass with an E^{-3} energy spectrum, "trigger" the detector with the simulated showers in Monte Carlo fashion, reconstruct the simulated showers with the same algorithm used to treat the experimental events, and then fit the experimentally observed X_{\max} distribution with some combination of the simulated sets. The best fit shows the cosmic ray composition.

Technically the Monte Carlo simulation is divided into two parts: a shower Monte Carlo and a detector Monte Carlo. The shower Monte Carlo implements the high energy physics input, simulates the shower development in the atmosphere and calculates the number of charged particles in individual showers as a function of the atmospheric depth. Since there are no accelerator measurements at the energies involved (which in the center of mass of the interacting nuclei are near those of the SSC) the particle physics input is determined by the interpretation of measurements at lower energy and their extrapolation. For the purposes of this work we have used three different particle physics models tuned to reproduce equally well the main observed features of high energy hadronic interactions. These are the statistical model,¹⁹ a QCD Pomeron model,²⁰ and the QCD mini-jet model.²¹

The detector Monte Carlo simulates the triggering conditions and the detector response. It uses showers created by the shower Monte Carlo as input. In the shower Monte Carlo, each shower is assigned a random direction, zenith angle and impact distance to the detector. The amount of light is calculated as a function of the atmospheric depth as a sum of the nitrogen fluorescence and direct and scattered Cherenkov radiation. Solid angle effects and light extinction due to atmospheric Rayleigh and aerosol scattering are taken into account. The optical and electronic characteristics of the detectors are modeled to calculate the photoelectron pulse in each phototube. The output consists of a list of triggered phototubes with their timing and amplitude information, exactly like

data from real events. This output is finally analyzed using the standard analysis technique¹⁷ to generate a sample of simulated events corrected for the triggering efficiency, acceptance and reconstruction resolution of the detector.

The set of Monte Carlo programs was used to study the sensitivity of the data analysis to different assumptions used in the reconstruction program, and of the final results to different particle physics input. A full description of the data analysis technique is given in Cassidy *et al.*¹⁷ and Gaisser *et al.*²² In the latter paper we examine the uncertainties possibly introduced by different stages of the simulation and data analysis algorithms and we discuss in more detail the different models of hadronic interactions we have used. The estimated experimental systematic shift in X_{\max} is not more than 20 g/cm^2 and the estimated systematic shift in the Monte Carlo predictions is 10 g/cm^2 . As in Ref. 22, the Monte Carlo predictions have been shifted by -25 g/cm^2 , since otherwise even iron nuclei could not account for the early rise of the experimental X_{\max} distribution. This shift is consistent with the systematic uncertainty and does not change the qualitative conclusions on the composition of cosmic rays. The current detector resolution in X_{\max} is $\pm 45 \text{ g/cm}^2$. Since the expected separation in X_{\max} between H and Fe is $\sim 100 \text{ g/cm}^2$, our present results should be considered preliminary, and should be confirmed by a higher resolution detector such as the High Resolution Fly's Eye.²³ The derived cosmic ray composition is, however, extremely interesting and may have broad astrophysical implications, which we discuss below.

3. EXPERIMENTAL RESULTS

The data set used in this analysis consists of 2529 showers of energy above $3 \times 10^{17} \text{ eV}$ collected in 2649.1 hours of observation between November 1986 and June 1990. Only data in stereo (i.e., viewed simultaneously by both FE I and FE II) are used. The experimental cuts required good X_{\max} reconstruction (relative error in X_{\max} less than 12%), viewing angle between FE I and FE II greater than 20° , and small contamination by Cherenkov light.

The data set was divided into three groups of energy: $3-5 \times 10^{17}$, $5-10 \times 10^{17}$ and $>10^{18} \text{ eV}$. The composition fits were per-

TABLE I

Results from the composition fit. Column 4 gives the all particle flux measured by the Fly's Eye. Energy is in units of EeV (10^{18} eV). The χ^2 values are per degree of freedom.

E EeV	#	$\langle E \rangle$ EeV	$E \times J$ $\text{cm}^{-2}\text{s}^{-1}\text{sr}^{-1}$	Composition Fit			Pure Beam χ^2		
				H	Fe	χ^2	H	CNO	Fe
0.3-0.5	994	0.38	2.5×10^{-15}	0.21 ± 0.07	0.79 ± 0.11	2.51	101.	15.8	10.4
0.5-1.0	867	0.63	8.8×10^{-16}	0.27 ± 0.12	0.66 ± 0.12	1.56	43.1	12.5	9.3
>1.0	690	1.41	1.7×10^{-16}	0.43 ± 0.04	0.56 ± 0.05	0.96	12.5	4.1	7.7

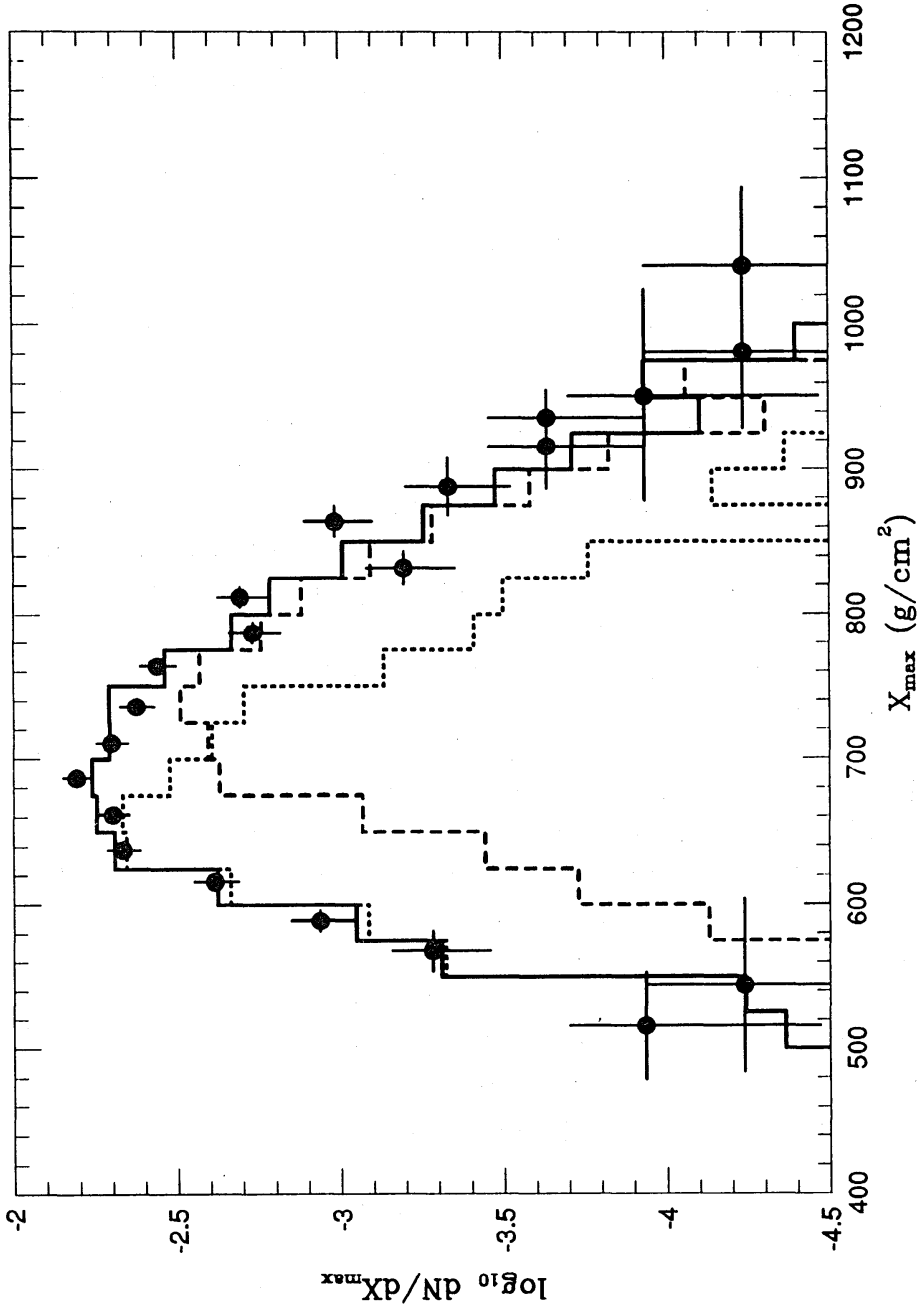


FIGURE 1 Comparison of the fitted depth of maximum distribution (histogram) to experimental data for showers of energy above 10^{18} eV. The dashed histogram shows the contribution of the light (H + He) component and the dotted one shows the contribution of the heavy component. The fit used the KNP (Ref. 20) model of hadronic interactions.

formed with a χ^2 minimization procedure using for each energy set three sets of simulated showers, generated by H, C, and Fe primaries. The results of the fits are given in Table I for the KNP particle interaction model, which gives the best overall fits. The table also shows the preliminary all particle flux measured²⁴ by the Fly's Eye experiment and the χ^2 values for fits with pure H, C and Fe cosmic ray beams. Figure 1 shows the comparison of the fitted X_{\max} distribution to the experimental one for showers of energy greater than 10^{18} eV.

The calculations were done using H, C, and Fe components to approximate the more complicated actual composition. This is justified by considering the experimental resolution in X_{\max} (45 g/cm²) and the fact that X_{\max} varies slowly (approximately logarithmically) with A , the atomic weight. Previous simulations²⁵ have shown that H and He are not distinguishable at this energy, because their cross sections for inelastic collisions in the atmosphere are almost identical. Thus, the H component approximates the combined effect of H and He. Similarly, elements in the vicinity of the CNO group are approximated by the C component and heavier elements are approximated by the Fe component.

The disagreement of the experimental data points with the assumption of a pure composition is obvious from an inspection of the reduced χ^2 values in Table I. It is interesting to notice, though, that the χ^2 value for a pure proton composition is very strongly energy dependent. The lowest χ^2 is the one for pure C at $E > 10^{18}$ eV. At this energy the C component peaks in the X_{\max} distribution at the same depth as the data do, and the χ^2 value reflects the insufficient width of the distribution. The mixed composition fits generally show a much better fit to the data, although they are obviously worse in the lowest energy bin, which might be a reflection of less precise modeling of the detector close to its energy threshold. The biggest contribution to the χ^2 in this energy bin comes from showers that appear to develop earlier than the calculation for Fe.

Table I shows that the fitting program tends to neglect the C group. This happens because the fits need the Fe fraction to describe the rising edge of the X_{\max} distribution and the H fraction to describe its tail. The combined width of these two components is enough to describe the experimental distribution without the C

component which peaks between the other two components. When we fix the Fe fraction at a suitable value, we obtain a 3-component fit almost as good as the 2-component one. For the $E > 10^{18}$ eV group, e.g., fixing the Fe component at 40% leads to a normalized χ^2 minimum of 1.19 near 20% C and 40% H, the same fraction as the unrestricted fit yields. The comparison of these two fits emphasizes the conclusion that while the H fraction of the cosmic ray flux (plus an unknown contribution from He) is well measured, the Fe fraction in Table I might include a wide range of heavier nuclei, including some of the CNO group. Finally it should be mentioned that the other particle physics models which were tested require an even heavier composition in order to fit the data set.²²

4. DISCUSSION AND CONCLUSIONS

Table I shows a cosmic ray chemical composition (assuming the KNP model²⁰ of hadronic interactions), which is very heavy at energy above 3×10^{17} eV. It contains, however, an emerging light component that grows to $\sim 40\%$ of the total flux above 10^{18} eV. A separate analysis of the data also supports this conclusion. This analysis involves the measured elongation rate L_E . L_E is the rate of change of the average depth of maximum $\langle X_{\max} \rangle$ with energy, which should be close to constant at ~ 50 g/cm² per energy decade for constant composition. The data shows instead $L_E = 75 \pm 4$ g/cm², which is indicative of a composition that becomes lighter at higher energy. We conclude, therefore, that the cosmic ray composition is heavy at 3×10^{17} eV and that the composition becomes lighter at higher energies. It is interesting to test different theoretical models against these conclusions.

The results of our analysis are clearly inconsistent with models which predict very light composition for cosmic rays above the "knee." For example, they would constrain some of the models of Protheroe and Szabo¹⁶ which predict a flux of pure hydrogen generated by neutron leakage from active galactic nuclei. For their model in which the acceleration rate is highest and the radiation environment is most favorable for acceleration (curve *a* of Fig. 2 of Ref. 16) a proton flux could dominate from $\sim 3 \times 10^{15}$ to $\sim 10^{18}$ eV, and this appears to be ruled out by the data.

In a traditional²⁶ cosmic ray composition model, where every component goes through a rigidity dependent spectral break with $\Delta\gamma = 0.4$ one can estimate the enrichment of the cosmic ray flux with heavy nuclei. Assuming that all heavy nuclei are Fe and all light nuclei H, the maximum enrichment possible after the spectral break is $26^{0.4} = 3.7$. The observed ratio of the light (H + He) to the heavy ($A > 4$) component decreases from 3/2 at GeV energies to 1/4 at 3×10^{17} eV, a change by a factor of 6. Our data does not support models that explain the cosmic ray spectrum only with a rigidity dependent escape from the galaxy, although the current accuracy is not sufficient to rule them out completely.

Ip and Axford²⁷ propose a reacceleration of the cosmic ray flux at large scale galactic shocks (possibly groups of old supernova remnants, or superbubbles). There is no sharp bend and the spectral index changes continuously until a maximum acceleration energy E_{\max} is reached. With the restriction that the proton gyro-radius is smaller than 150 pc (to fit in the galactic disk) and an average magnetic field strength of 6 μ G, their calculation yields an exponential cutoff for the maximum acceleration energy (E_{\max}) for H of 3×10^{17} eV, i.e., at the lowest energy bin of the Fly's Eye data. At this energy they estimate that the cosmic ray beam is still dominated by hydrogen nuclei, which is inconsistent with our results. Our data do not allow for proton E_{\max} greater than $\sim(2-3) \times 10^{16}$ eV. At much lower energy the model of Ip and Axford is also inconsistent with the direct measurements of JACEE⁴ that already show a decrease of the H component at 10^{14} eV.

Völk and Biermann²⁸ have developed a model that accelerates particles beyond $10^{14} \times Z$ with blast shocks in the heavy and highly magnetized presupernova wind of exploding Wolf Rayet stars. For a magnetic field strength of 3 G at a fiducial distance of 10^{14} cm they obtain $E_{\max} = 10^{17} \times Z$ eV. This number would also be inconsistent with the results in Table I if the composition of the Wolf Rayet wind were not very heavy. Another feature of the same general model, developed recently in some detail by Biermann,²⁹ predicts both a rigidity dependent "bend" in the spectra of the accelerated nuclei (following from plasma physics considerations), and a cutoff. The additional "bend" energy parameter, limited by the theory only in order of magnitude to $\sim 10^{15}$ eV, brings the prediction to qualitative agreement³⁰ with our data.

We can use the numbers in Table I* to evaluate the emerging H flux. For $dN_p/d \ln E$ we find 5.3 ± 1.8 , 2.4 ± 1.1 , and $0.73 \pm 0.07 \times 10^{-16}$ per $\text{cm}^2 \cdot \text{s} \cdot \text{sr}$ at E equal to 0.38, 0.63 and 1.41 EeV, respectively. These numbers could be treated as an upper limit of the extragalactic flux of H (and He) nuclei. They give an exponent $\gamma = 2.5 \pm 0.4$ for a differential power law spectrum of the light cosmic ray component in the vicinity of 10^{18} eV, which is not inconsistent (bearing in mind a small but not insignificant galactic contribution) with a very flat ($\gamma = 2$) spectrum for the extragalactic component.

To emphasize this point we plot on Fig. 2 the three data points on top of models of extragalactic cosmic rays accelerated in AGN jets.³¹ The theoretical curves represent the sum of the contribution of all AGN including evolution and propagation effects. The thin lines represent spectra with $\gamma_{\text{diff}} = 2.1, 2.5$ and 2.8 , consistent with the experimental data. No additional renormalization of the theoretical model was performed. The model curves are in agreement with the three data points. The maximum acceleration energy for the three models is 3, 10 and 30×10^{20} eV. This model also explains why the extragalactic cosmic ray flux should be deficient in heavy nuclei. The composition of the ultra-high energy cosmic rays reflects the composition of the intergalactic medium, where the abundance of heavy nuclei is $\sim 1/3$ of the solar abundance.³¹ At very high energies nuclei suffer photodisintegration on the microwave background during propagation. The energy of 10^{18} eV is, however, too low³² for photodisintegration on the 3 K field.

All source injection spectra³¹ on Fig. 2 have $\gamma_{\text{diff}} = 2$ and the spectrum at earth is modified^{33,34} in interactions on the microwave background during propagation. The cutoff at 5×10^{19} eV (Greisen-Zatsepin cutoff) is due to photoproduction interactions $p + \gamma \rightarrow \Delta^+$. The interaction products cause the pile-up just below the cutoff. The plateau above 10^{18} eV is caused by energy loss in e^+e^- pair production. The energy range of the Fly's Eye is in the lower end of this region, where the modification of the injection spectrum is less significant. Although the predictions also depend on the

*The flux values in Table I are based (Ref. 24) on the preliminary results from a high statistics sample of mono (i.e., only observed by FE I) showers.

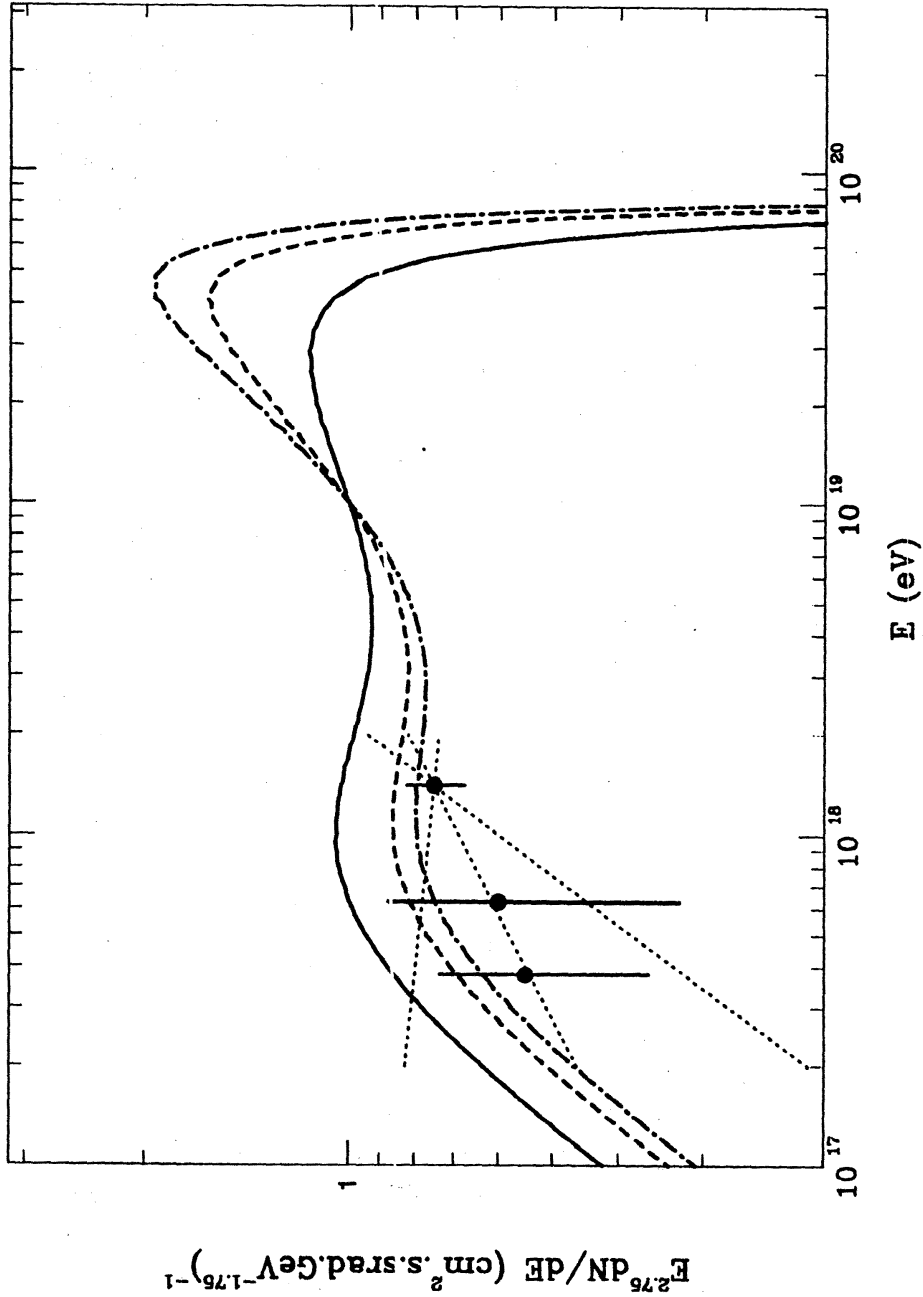


FIGURE 2 Comparison of the light cosmic ray component (H + He) derived from the composition fits to models from Ref. 31, which assume that protons are accelerated with a $\gamma = 2$ differential spectrum to a maximum energy of 3×10^{20} eV (solid), 10^{21} eV (dash) and 3×10^{21} eV (dash-dot). Thin dotted lines show the shape of the emerging light cosmic ray component.

intergalactic diffusion coefficient, which determines the propagation time from the sources to the vicinity of the earth, our results are still somewhat sensitive to the extragalactic source spectrum.

In summary, we have measured the chemical composition of the cosmic rays at energies around 10^{18} eV. We observe a composition rich in heavy nuclei in agreement with direct data at 10^{14} eV and with the conclusions from the analysis of some types of air shower data.⁸⁻¹¹ These *composition* results are consistent with models that require a change of slope of the “knee” component at about $\approx (2-4) \times 10^{14} \times Z$ eV. Higher values are allowed if the “knee” component has an inherently heavy composition. We also detect a light component, consisting of hydrogen and possibly helium nuclei, which increases with energy to about 40% of the flux of all particles above 10^{18} eV. This component has a distinctly different spectral index, much flatter than the shape of the all particle cosmic ray spectrum, which may signal the emergence of an extragalactic cosmic ray component. The absolute value of this light component is consistent with the model of Rachen and Biermann²⁹ for particle acceleration in AGN jets.

Acknowledgments

We are thankful to Dr. R. J. Protheroe for a clarification of the models of Ref. 16. We would like to acknowledge the support of the National Science Foundation in independent grants to the Fly’s Eye Experiment and to T.K.G. and T.S. The research of D. J. Bird is supported in part by DOE.

T. K. GAISSER, TODOR STANEV and SERAP TILAV†
*Bartol Research Institute,
 University of Delaware,
 Newark, Delaware 19716*

S. C. CORBATO, H. Y. DAI, B. R. DAWSON,††
 J. W. ELBERT, B. EMERSON,††† D. B. KIEDA,

†Present address: Department of Physics, University of Wisconsin, Madison, WI 53706.

††Present address: Department of Physics and Mathematical Physics, University of Adelaide, Adelaide, South Australia 5001.

†††Present address: Science Department, Central Oregon Community College, 2600 NW College Way, Bend, OR 97701.

M. LUO, S. KO, C. LARSEN, E. C. LOH,
M. H. SALAMON, J. D. SMITH, P. SOKOLSKY,
P. SOMMERS, J. TANG and S. B. THOMAS

*Department of Physics,
University of Utah,
Salt Lake City, Utah 84112*

D. J. BIRD
*Physics Department,
University of Illinois,
Urbana, Illinois 61801*

References

1. J. J. Engelmann *et al.*, *Astron. Astrophys.* **233**, 96 (1990).
2. S. P. Swordy *et al.*, *Ap. J.* **349**, 625 (1990).
3. K. Asakimori *et al.*, in *Proc. 22nd Int. Cosmic Ray Conf., Dublin, Ireland* (Dublin Institute for Advanced Studies, Dublin, Ireland, 1991), vol. 2, p. 57.
4. K. Asakimori *et al.*, in *Proc. 22nd Int. Cosmic Ray Conf., Dublin, Ireland* (Dublin Institute for Advanced Studies, Dublin, Ireland, 1991), vol. 2, p. 97.
5. S. I. Nikolskii, in *Cosmic Rays and Particle Physics*, eds. A. Oshawa and T. Yuda (Institute for Cosmic Ray Research, Tokyo, 1984), p. 507; V. G. Denisova *et al.*, in *Proc. 20th International Cosmic Ray Conference, Moscow, 1987*, eds. V. A. Kozyarivsky *et al.* (Nauka, Moscow, 1987), vol. 1, p. 390.
6. C. E. Fichtel and J. Linsley, *Ap. J.* **300**, 474 (1986).
7. S. Alen *et al.*, *Phys. Rev. D* **46**, 895 (1992).
8. G. B. Yodh *et al.*, *Phys. Rev. D* **29**, 892 (1984).
9. J. R. Ren *et al.*, *Phys. Rev. D* **38**, 1404 (1988).
10. H. T. Freudenreich *et al.*, *Phys. Rev. D* **41**, 2732 (1990).
11. E. Chatelet, T. V. Danilova, A. D. Erlykin and J. Procureur, in *Proc. 22nd Int. Cosmic Ray Conf., Dublin, Ireland* (Dublin Institute for Advanced Studies, Dublin, Ireland, 1991), vol. 2, p. 45.
12. R. D. Blandford and D. Eichler, *Phys. Reports* **154**, 1 (1987).
13. L. O'C. Drury, *Rept. Prog. Phys.* **46**, 973 (1983).
14. P. O. Lagage and C. J. Cesarsky, *Astron. Astrophys.* **125**, 249 (1983).
15. J. Wdowczyk and A. W. Wolfendale, *Ann. Rev. Nucl. Part. Sci.* **39**, 43 (1989).
16. R. J. Protheroe and A. P. Szabo, *Phys. Rev. Lett.* **69**, 2885 (1992).
17. G. L. Cassiday *et al.*, *Astrophys. J.* **356**, 569 (1990).
18. R. M. Balrusaitis *et al.*, *Nucl. Inst. Meth. A* **240**, 410 (1985).
19. See, e.g., G. N. Fowler *et al.*, *Phys. Rev. D* **35**, 870 (1987).
20. B. Z. Kopeliovich, N. N. Nikolaev and I. K. Potashnikova, *Phys. Rev. D* **39**, 769 (1989).
21. T. K. Gaisser and F. Halzen, *Phys. Rev. Lett.* **54**, 1754 (1987); L. Durand and H. Pi, *Phys. Rev. Lett.* **58**, 303 (1987); T. K. Gaisser and T. Stanev, *Phys. Lett.* **219B**, 375 (1989).
22. T. K. Gaisser *et al.*, *Phys. Rev. D* (in press).
23. E. C. Loh *et al.*, *Astrophysical Aspects of the Most Energetic Cosmic Rays*, eds. M. Nagano and F. Takahara (World Scientific, Singapore, 1991), p. 345.

24. P. Sokolsky, P. Sommers and B. R. Dawson, *Phys. Reports* (in press).
25. R. W. Ellsworth *et al.*, *Phys. Rev. D* **26**, 336 (1982).
26. B. Peters, *Il Nuovo Cimento* **22**, 800 (1961).
27. W. H. Ip and W. I. Axford, in *Particle Acceleration in Cosmic Plasmas*, eds. G. P. Zank and T. K. Gaisser (AIP Conference Proceedings 264, 1992), p. 400.
28. H. J. Völk and P. L. Biermann, *Ap. J. Lett.* **333**, L65 (1988).
29. P. L. Biermann, *Astron. Astrophys.* (in press).
30. T. Stanev, P. L. Biermann and T. K. Gaisser, submitted to *Astron. Astrophys.*
31. J. Rachen and P. L. Biermann, *Astron. Astrophys.* (in press).
32. J. L. Puget, F. W. Stecker and J. H. Bredekamp, *Astrophys. J.* **205**, 638 (1976).
33. C. T. Hill, D. N. Schramm and T. P. Walker, *Phys. Rev. D* **36**, 1007 (1987).
34. V. S. Berezinsky and S. I. Grigor'eva, *Astron. Astrophys.* **199**, 1 (1988).